

Magnetic Field-Sensitive Radical Pair Dynamics in Polymethylene Ether-Bridged Donor–Acceptor Systems

Hao Minh Hoang,^{†,‡} Van Thi Bich Pham,[‡] Günter Grampp,[‡] and Daniel R. Kattnig^{*,§}

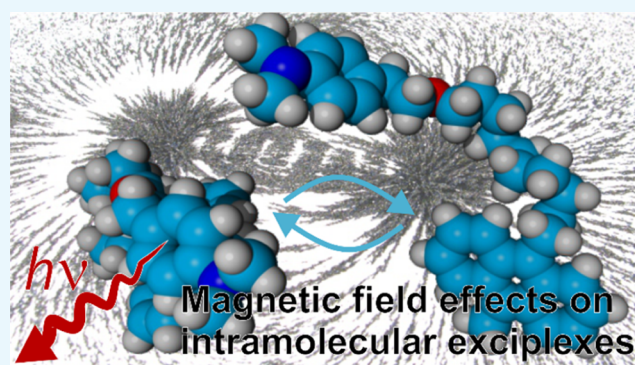
[†]Ho Chi Minh City University of Technology and Education, Vo Van Ngan 01, Linh Chieu Ward, Thu Duc District, Ho Chi Minh City 700000, Vietnam

[‡]Institute of Physical and Theoretical Chemistry, Graz University of Technology, Stremayrgasse 9/I, A-8010 Graz, Austria

[§]Living Systems Institute and Department of Physics, University of Exeter, Stocker Road, Exeter, Devon EX4 4QD, United Kingdom

Supporting Information

ABSTRACT: Donor–acceptor systems forming exciplexes are versatile models for the study of magnetic field effects (MFEs) on charge recombination reactions. The MFEs originate from singlet–triplet interconversion within transient radical ion pairs (RIPs), which exist in a dynamic equilibrium with the exciplexes. Here, we describe the synthesis and MFEs of the chain-linked *N,N*-dimethylaniline (DMA)/9-methylanthracene (MAnt) donor–acceptor system MAnt–(CH₂)_{*n*}–O–CH₂–CH₂–DMA for *n* = 6, 8, 10, and 16. The MFEs are found to increase with increasing chain length. Effects as large as 37.5% have been observed for the long-chain compound with *n* = 16. The solvent dependence of the MFEs at magnetic field intensity 75 mT is reported. For the range of solvent static dielectric constants $\epsilon_s = 6.0$ –36.0, the MFEs go through a maximum for intermediate polarities, for which the direct formation of RIPs prevails and their dissociation and reencounter are balanced. Field-resolved measurements (MARY spectra) are reported for solutions in butyronitrile. The MARY spectra reveal that for *n* = 8, 10, 16, the average exchange interaction is negligible during the coherent lifetime of the radical pair. However, singlet–triplet dephasing broadens the lineshape; the shorter the linker, the more pronounced this effect is. For *n* = 6, a dip in the fluorescence intensity reveals a nonzero average exchange coupling of the order of ± 5 mT. We discuss the field-dependence in the framework of the semiclassical theory taking spin-selective recombination, singlet–triplet dephasing, and exchange coupling into account. Singlet recombination rates of the order of 0.1 ns^{−1} and various degrees of singlet–triplet dephasing govern the spin dynamics. In addition, because of a small free energy gap between the exciplex and the locally excited fluorophore quencher pair, a fully reversible interconversion between the RIP, exciplex, and locally excited fluorophore is revealed by spectrally resolved MFE measurements for the long-chain systems (*n* = 10, 16).



INTRODUCTION

Exciplexes are excited-state charge-transfer complexes that can be formed in photo-induced electron-transfer (PET) reactions in moderately polar solutions. Magnetic field effects (MFEs) on the emission of exciplexes have been extensively studied for many years.^{1–16} The MFEs result from the magnetic field-dependent intersystem crossing within the fully charge-separated radical ion pairs (RIPs) in equilibrium with the exciplexes (see Figure 1). By systematically studying the MFE of the exciplex emission, details of the dynamics of the spin-correlated RIP can be revealed indirectly.^{5,6,9–11} The MFEs are theoretically accounted for in the framework of the so-called *radical pair mechanism*.^{4,12,13,17–20} It relies on the quantum-coherent mixing, by the hyperfine interaction (HFI) and its interplay with the Zeeman interaction, of the singlet (S) and three triplet sublevels (T_±, T₀) describing the spin configurations of the two uncompensated electron spins on the radical ions (hyperfine mechanism). Specifically, for high

magnetic field intensities, the degree of singlet–triplet mixing is reduced as the magnetic field lifts the degeneracy of the triplet and singlet states (see Figure 2a), thereby reducing the number of states accessible to spin mixing. As a consequence, the singlet–triplet conversion is impeded and the yield of the charge-recombination products accessible from the singlet radical pair, such as the exciplex, increases. For moderate field intensities, the alternative Δg -mechanism is typically irrelevant as the difference in the Larmor precession frequencies of the two radicals, $\mu_B \Delta g B_0 / \hbar$, is small compared with their inverse lifetime. Figure 1 depicts a comprehensive reaction scheme of an intramolecular PET processes in an exciplex-forming fluorophore-bridge-quencher system with flexible linker. The ordinate symbolizes free energy and the abscissa corresponds

Received: June 4, 2018

Accepted: August 20, 2018

Published: August 31, 2018

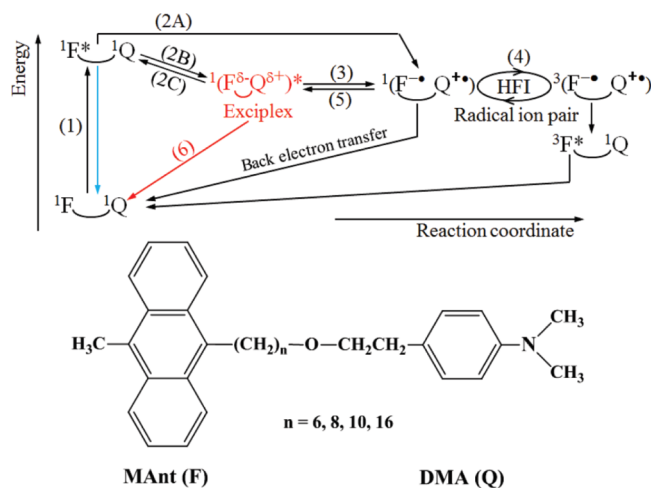


Figure 1. Reaction scheme underlying the MFEs of an intramolecular, exciplex-forming donor–acceptor systems at weak-to-moderate field intensities. The pertinent reaction steps are (1) photoexcitation, (2A) direct RIP formation by distant ET, (2B) exciplex formation, (2C) reversible inter-conversion of the exciplex to the locally excited fluorophore–quencher pair, (3) exciplex dissociation into RIP, (4) singlet–triplet interconversion by the HFI, (5) reformation of the exciplex from the singlet ion pair, and (6) exciplex emission. The blue and red arrows refer to the, in part radiative, decay processes of the locally excited fluorophore and the exciplex, respectively. Spin multiplicities are indicated by superscripts.

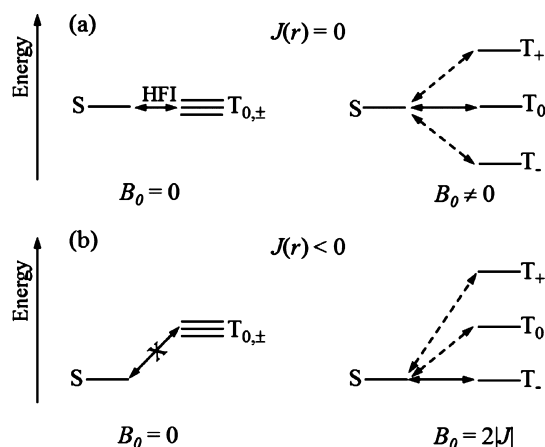


Figure 2. Graphic visualization of the relative energies of the S- and T-states that govern the ISC efficiency for $B_0 = 0$ (left) and in the presence of an external magnetic field for systems without [(a) $J(r) = 0$] and with sizeable, negative [(b) $J(r) < 0$] exchange coupling. Assuming that the HFIs are small on the drawn scale, which is usually the case, efficient intersystem crossing depends on the approximate degeneracy of the S- and T-states.

to a projection of a two-dimensional reaction coordinate, which comprises the interparticle distance and the solvent polarization in the form of the Marcus outer-sphere electron-transfer (ET) coordinate.^{8,9} See refs^{9,11,21–23} for a discussion of various reaction pathways. These studies mostly pertain to intermolecular systems. The notable exception is the work of Zachariasse and co-workers detailing the effect of the bridge on the free-energy difference of exciplex and ion-pair in a linked anthracene/amine exciplex system.²³ Together, these studies suggest that the relative importance of the quenching pathways 2A and 2B in Figure 1 is expected to vary with chain length and solvent polarity.

The degree and characteristics of the magnetosensitivity of the RIP depend on the strength of the exchange interaction of the two radicals. By energetically splitting singlet from triplet states, the primary effect of this interaction is to suppress MFEs (see Figure 2b; left scenario).²⁴ As the exchange integral $J(r)$ decreases approximately exponentially with the inter-radical distance r , $J(r) = J_0 \exp(-\xi r)$, large MFEs are often dependent on the diffusive separation of the two radicals (followed by their reencounter and recombination for product formation). Typically, $\xi \approx 0.4 \text{ nm}^{-1}$ while J_0 varies from system to system.¹⁸ Consequently, for distances of the order of tens of angstroms the exchange interaction falls off to zero,¹⁸ and the degeneracy of the singlet and three triplet states (in the absence of an external magnetic field) enable MFEs as described in the previous paragraph. Alternatively, if the radical pair experiences a nonzero exchange interaction, significant MFEs can still occur if the external magnetic field is able to re-establish the near-degeneracy of T_+ (or T_- , depending on the sign of J) and the S states, for which hyperfine-induced spin mixing is again efficient (see Figure 2b; right scenario). For charge-transfer systems studied here, $J(r)$ can be estimated from ET properties such as the charge recombination free energy, the reorganization energy, the energy of the locally excited triplet state, and the electron coupling matrix element.^{8,25} In this case, the distance dependence of $J(r)$, that is, the ξ -parameter, predominantly reflects the distance dependence of (the square of) the ET coupling matrix element. For the *N,N*-dimethylaniline (DMA)/9,10-dimethylanthracene (DMAnt)-based system studied here, J is predicted to be negative (following the convention as expressed in eq 2 below), that is, the scenario as shown in Figure 2b is likely relevant.⁸

The relative diffusive motion of the radicals plays an important role for the sizes of the MFEs of exciplexes. In several studies, the solvent environment was varied to control this factor via the static dielectric constant (ϵ_s) and the dynamic viscosity (η).^{5,6,8–11,26–30} In nonpolar solvents, the spin mixing and, thus, MFEs are often found to be impeded by the inability of the radical pair to separate to a distance for which J is small. If, on the other hand, the solvent polarity is high, the diffusive separation might be efficient. Yet, for intermolecular systems, the MFEs may still be small if the reencounter probability of the geminate radicals is small. Consequently, maximal MFEs are often observed for intermediate dielectric constants, for which the solvent polarity is chosen to balance the radical separation and the reencounter probability.^{5,6,9–11} In micro-heterogeneous solvent mixtures, these parameters can in addition be controlled via the solvent structure, which can be optimized to elicit very large MFEs.^{5,6,11}

For bridged intramolecular exciplex systems, the radicals cannot separate freely and interesting MFEs are expected to emerge based on the interplay of the exchange interaction and the radical dynamics as confined by the bridge and steric requirements. In particular, by interconnecting the fluorophore and the quencher moieties with a flexible linker, the diffusive excursion of the radicals and their limiting distances and thus the average exchange integral can be controlled. By choosing a suitable chain length, MFEs that markedly exceed those in freely diffusing systems have been realized. For pyrene– $(\text{CH}_2)_m$ –DMA with $m = 16$, MFEs of approximately 45% have been reported.³¹ For linkers with $m \leq 8$, the effect of the exchange interaction is pronounced.^{32–40} In contrast to

intermolecular systems and the long-chain analogues, dips in the MFE versus magnetic field-curves are then observed as a result of the S–T_±-mixing process for nonzero average J (i.e., as predicted by Figure 2b; right scenario). So far, MFEs have only been observed for two classes of intramolecular exciplex systems: pyrene/DMA^{30–32} and phenanthrene/DMA.^{33–38} MFEs in nonexciplex forming intramolecular radical pair systems are comparably well studied.^{17,41–44}

In this work, we describe the synthesis and MFEs of a new class of exciplex-forming donor–acceptor systems of the type 9-methylanthracene (MAnt)–(CH₂)_{*n*}–O–CH₂–CH₂–DMA, which feature chain-linked MAnt and DMA. The MFEs of these compounds were studied using steady-state recordings of the exciplex emission. The chain length and solvent polarity dependence of the MFEs was investigated in homogenous binary solvent mixtures of propyl acetate (PA) and butyronitrile (BN) with widely varying dielectric constants, ϵ_s , in the range from 6 to 24.7 (at 295 K; $\eta = 0.58$ cP). Propionitrile (EtCN; $\epsilon_s = 28.3$; $\eta = 0.39$ cP) and acetonitrile (AN; $\epsilon_s = 36.0$; $\eta = 0.34$ cP) were used to extend the solvent polarity range. We model the field-dependence in the framework of the semiclassical approximation and demonstrate under which conditions a model employing ST-dephasing rather than a microscopic description of the chain dynamics is sufficient to account for the MFEs.

RESULTS AND DISCUSSION

Permittivity-Dependent MFE on Exciplex Emission.

Figure 3 depicts the normalized absorption and fluorescence

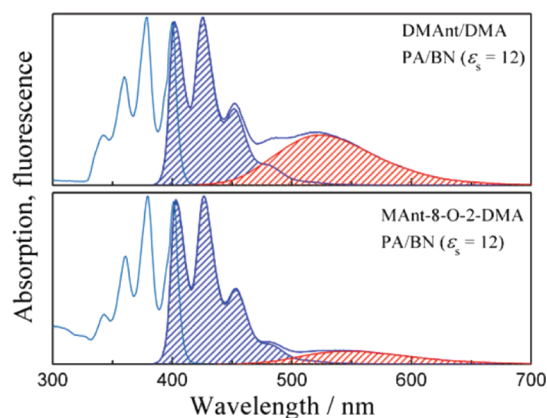


Figure 3. Absorption and emission spectra of DMAnt/DMA (top; quencher concentration: 0.06 M) and MAnt-8-O-2-DMA (bottom). A mixture of PA/BN with a dielectric constant of $\epsilon_s = 12$ was used as solvent. The emissions of the locally excited fluorophore moiety and the exciplex are shaded in blue and red, respectively.

spectra of MAnt-*n*-O-2-DMA and, for comparison, the intermolecular system DMAnt/DMA. The vibronic transitions with Gaussian band shape of the exciplex were extracted by employing a model as described in refs.^{8,45} The fluorescence spectrum of the locally excited fluorophore was directly accessible from the spectrum in the absence of the quencher moiety.

Figure 4 shows the MFEs of the exciplexes of the chain-linked MAnt-*n*-O-2-DMA systems ($n = 8, 10, 16$) in PA/BN mixtures, propionitrile (EtCN), and AN and compares them to the effects observed for a freely diffusing system, which are available from a previous study.^{9–11} We have not studied the

permittivity dependence of the $n = 6$ compound in detail as the MFE was found to be very small ($\chi_E = 1.0\%$ in BN; see below). The MFEs have been determined from steady-state measurements at $B_0 = 75$ mT and the Earth's magnetic field ($B_0 \approx 0$ mT) and corrected for background fluorescence as detailed in eq 8. The used PA/BN binary mixtures are isoviscous and, thus, allow a systematic assessment of the static dielectric constants of the solvents, ϵ_s , unmitigated by effects of diffusivity. For the freely diffusing donor–acceptor pair, no MFE has been observed for $\epsilon_s < 7$. For $\epsilon_s > 7$, the MFE increases sharply and eventually assumes a maximum value of $\chi_E = 14.5\%$ at $\epsilon_s = 18$, followed by a monotonous decrease for $\epsilon_s > 18$. For the polar solvents EtCN and AN, the emission of the intermolecular exciplex is too weak to allow a reliable quantification of the MFE. These data points have thus been omitted. For the linked systems, the onset of the MFEs is observed for $\epsilon_s \approx 10$ and the effect steadily increases with increasing dielectric constant in the PA/BN mixtures. Independent of the chain length, the maximal effect is observed for pure BN, $\epsilon_s = 24.7$, for which we find $\chi_E = 9.4\%$ for MAnt-8-O-2-DMA, $\chi_E = 17.8\%$ for MAnt-10-O-2-DMA and $\chi_E = 37.5\%$ for MAnt-16-O-2-DMA. Eventually, the MFE is markedly lower for the more polar solvents EtCN and AN. In this respect, our results differ from those for methylene-linked pyrene/DMA, for which the MFE on the exciplex was found to increase in ethyl acetate/AN mixtures up to $\epsilon_s = 37.5$, that is, pure AN, without going through a maximum.^{26,30} On

the other hand, a very similar permittivity dependence of the MFE was observed for polymer-chain-linked pyrene–dimethylaniline in tetrahydrofuran/dimethylformamide mixtures.¹³ Our observations can be understood as follows: MFEs of exciplexes originate from the hyperfine-induced intersystem crossing of RIPs, which may be produced directly in a PET reaction or via dissociation of the exciplex (see Figure 1). Only if the component radicals of the RIP can separate to distances for which the exchange interaction, $J(r)$, is negligible compared with the HFIs or, in the case of S–T_±-mixing, comparable to the Zeeman interaction, can the spin evolution proceed efficiently. The increase of the MFE with increasing ϵ_s is usually interpreted in terms of the accessibility of these magnetosensitive, that is, separated or elongated, conformers/states:^{9–11} first, as we have shown by a detailed analysis of the time-resolved MFEs of DMAnt/DMA, the propensity for the system to directly form the exciplex from the locally excited singlet state increases with decreasing ϵ_s , whereas the tendency of the exciplex to dissociate into ions decreases. Taken together, this gives rise to a larger partition of exciplex formation via magnetic field-independent pathways, a consequence of which is that the MFE is decreased. Second, even if RPs are formed, low permittivities/high viscosities will impede the separation of the radicals to distances that allow favorable ISC and thus large MFEs. As for the decrease of the MFE for EtCN ($\eta = 0.39$ cP) and AcN ($\eta = 0.34$ cP), we observe that these solvents are less viscous than the PA/BN mixtures ($\eta = 0.58$ cP).^{9–11} The associated increase in mobility is, however, not expected to account for the decrease in the MFE. In fact, model calculations employing the stochastic Liouville equation to incorporate the chain dynamics and the distance dependence of the exchange interaction and back ET rate suggest that for systems for which the average exchange interaction is not substantial, the MFE increases with increasing mobility (see Figure 4 in ref 30). On the other hand, the decrease in the MFEs can be attributed to altered

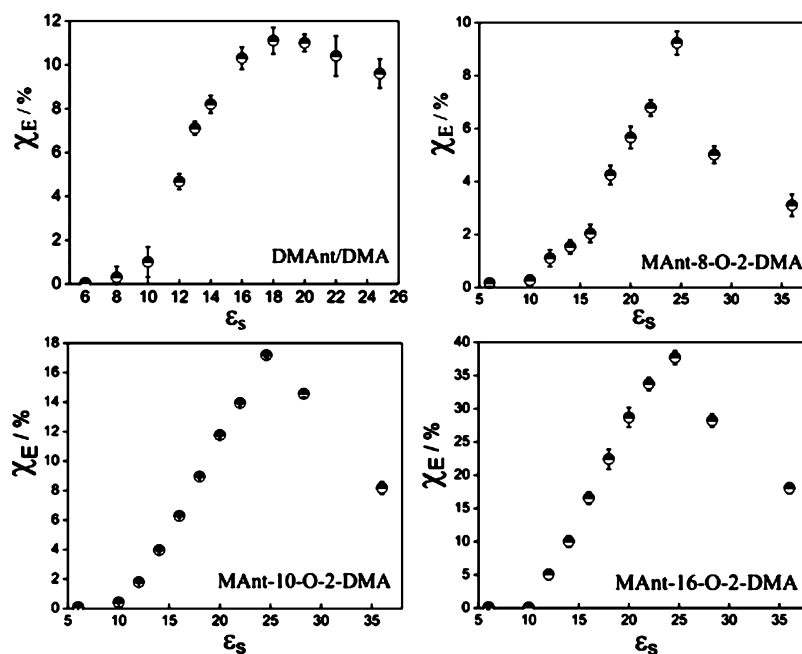


Figure 4. MFEs on the exciplexes from freely diffusing DMAnt/DMA and chain-linked MAnt-*n*-O-2-DMA as determined from steady-state-luminescence measurements (semi-filled circles with error bars) in PA/BN mixtures of various static dielectric constants ($\epsilon_s = 6 \div 24.7$) and neat propionitrile ($\epsilon_s = 28.3$) and AN ($\epsilon_s = 36.0$).

back ET rates (see Figure 1). Further, the reencounter rate of the separated radicals could be decreased with increasing permittivity because of increased charge shielding, such that the pair loses its spin coherence (or is quenched by impurities) prior to its reencounter.¹³ In this case, the magnetosensitivity will be suppressed, as the magnetic field is too weak to impact upon the equilibrium properties. This argument is frequently employed in the context of freely diffusing radical pairs.^{7,12,46} Together with the increasing accessibility of the magnetosensitive conformers discussed above, a maximum in the permittivity dependence of the MFE is expected and in fact observed. The maximum MFE values in the polymethylene ether-linked systems with long chains ($n = 10, 16$) are larger than the freely diffusing systems.^{9–11} This can be predominantly attributed to an increased probability of geminate radical-pair recombination in the bridged systems. For the short-chain systems, the effects of the exchange interaction are expected to become more significant such that the MFEs are reduced despite enhanced recombination probabilities. In addition, the flexible linker is expected to impact the ratio of direct exciplex versus RIP formation.²³ Magnetic field-dependent measurements to be reported below suggest that for $n = 8, 10,$ and 16 , the second argument applies exclusively.

Magnetic Field-Dependent Measurements. We have further studied the MFEs of the exciplexes for MAnt-*n*-O-2-DMA as a function of the magnetic field intensity, B_0 . Figure 5 summarizes our results for neat BN. For $n = 8, 10,$ and 16 , the MFE increases monotonously with B_0 , which is in line with the radical pair mechanism in the absence of a marked low-field effect. In particular, the spectral response suggests a short-lived radical pair that does not experience a significant exchange coupling during the diffusive excursions that determine the MFEs. In this scenario, the MFE encompasses the coherent mixing of the degenerate singlet (S) and triplet states (T_+, T_0, T_-) at $B_0 \approx 0$ mT and S- T_0 conversion at high-fields, for which the T_+ and T_- states are energetically detached by the

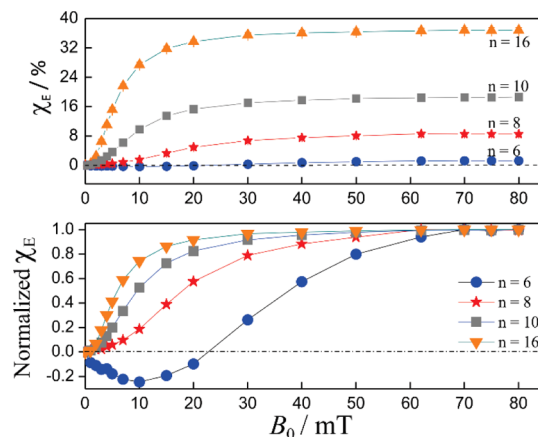


Figure 5. Dependence of the MFEs of the exciplex (χ_E ; see eq 8) of the polymethylene-linked compounds MAnt-*n*-O-2-DMA with $n = 6, 8, 10,$ and 16 on the external magnetic field intensity. The MFEs were obtained by steady-state measurements of the exciplex emission intensity at 550 nm using neat BN as solvent. The bottom panel shows the MFEs normalized by their respective value at 80 mT.

Zeeman interaction. For the comparable model system of methylene-linked pyrene/DMA, 12 or 11 intervening CH_2 -groups are necessary to similarly alleviate obvious extrema due to a nonzero exchange coupling in AN and diethyleneglycol, respectively.^{26,30} As for MAnt-8-O-2-DMA comprises 11 atoms (10 methylene groups and an ether oxygen atom), the two families of compounds appear very similar. We have further extracted the $B_{1/2}$ -values, that is, the magnetic field values for which the delayed exciplex fluorescence reaches half of its saturation relative to $B_0 = 0$ mT; for $n = 8, 10,$ and 16 , we determine this to be 18, 9.5, and 5.6 mT, respectively. We observe that for $n = 8$ and 10 , the $B_{1/2}$ -values are markedly larger than the corresponding value for the free fluorophore-quencher-pair DMAnt/DMA in the limit of low donor

concentration ($B_{1/2} = 5.3$ mT).^{5,6} This can be attributed to a reduced lifetime of the radical pair and/or singlet–triplet dephasing. In fact, the lifetime effect has been suggested to lead to a broadening of the MARY lines in a study of the micro-heterogeneous solvation of the radical pair of DMAnt/DMA in DMSO/toluene mixtures, which likewise promote large MFEs by increasing the reencounter probability.⁶ Singlet–triplet dephasing is the consequence of the randomization of the S/T-coherences by a time-varying $J(r)$ as caused by the molecular motion.^{5,6,47} Given that for $n \geq 8$, no spectral fingerprints of an average exchange coupling are revealed in Figure 5, the picture of brief random encounters with large exchange coupling, interrupted by comparably long stretches of “free” evolution, emerges. We note again that the exchange interaction decays exponentially with the distance between two radicals. In the freely diffusing DMAnt/DMA system, two radicals can separate freely to the region where the exchange interaction is negligible during the majority of the coherent RP lifetime such that its effect can be neglected. The fact that for $n = 16$, the $B_{1/2}$ -parameter is only marginally larger than for the freely diffusing system suggests that for this system, most of the diffusive excursion is taking place outside the mutual sphere of influence of the donor–acceptor pair, despite the linker. For the short-chain variant with $n = 6$, a completely different picture emerges: the MARY-spectrum shows a pronounced tip with negative MFEs at $B_0 \approx 10$ mT with an amplitude that amounts to approximately -20% of the saturated effect. The subsequent zero-crossing occurs at $B_0 \approx 23$ mT. This spectrum reflects a nonzero average exchange interaction, which lifts the degeneracy of the S- and T-states for $B_0 = 0$. As a consequence of this large S–T energy gap, HFI-induced intersystem crossing is inefficient for $B_0 = 0$ (Figure 2b). By applying an external magnetic field matching the S–T energy gap, the degeneracy of the T_+ -state and the S-state is restored (Figure 2b, right scenario). The once more efficient conversion of singlet to triplet RPs is revealed by the dip in the exciplex luminescence intensity. In this discussion, we have assumed that $J(r)$ is negative (for the convention as expressed by eq 2 below) in agreement with predictions from ref 8. A positive value has been suggested for some RPs.^{18,35,48} In this case, T_+ and T_- swap roles without requiring a principal adjustment to the conclusion.

We shall present a preliminary analysis of the spin dynamics in the MAnt- n -O-2-DMA. Here, we focus on a description based on the single-site modified Liouville equation. The effect of fluctuations in the exchange interaction will be accounted for by introducing an effective spin dephasing term. More elaborate descriptions accounting for the dynamics of the linker and the distance dependence of the spin Hamiltonian and the back ET rate constants have been suggested^{30,44,49–51} but are beyond the scope of this work. In fact, given the multitude of unknown parameters fed into such calculations, a more detailed study of the photophysical parameters should precede any endeavor in this direction. We nonetheless argue that the simplified approach employed here is valuable. This statement is supported by the success of modeling-flexible biradicals by two-state models^{52–54} and the fact that the intermittently populated state of large J can be well-modeled in terms of singlet–triplet dephasing as demonstrated in ref 55. Following this approach, the equation of motion of the spin density matrix is

$$\frac{d}{dt}\hat{\rho}(t) = -i[\hat{H}, \hat{\rho}(t)]_- + \hat{K}\hat{\rho}(t) + \hat{R}\hat{\rho}(t) - \tau_{sc}^{-1}\hat{\rho}(t) \quad (1)$$

Here, \hat{H} is the spin Hamiltonian comprising the Zeeman, hyperfine, and the average exchange interaction

$$\hat{H} = \hat{H}_1 + \hat{H}_2 + J_{av} \left(2\hat{S}_1 \cdot \hat{S}_2 + \frac{\hat{1}}{2} \right) \quad (2)$$

with

$$\hat{H}_i = \frac{g_i \mu_B B_0}{\hbar} \hat{S}_{i,z} + \sum_k a_{i,k} \hat{S}_i \cdot \hat{I}_{i,k} \quad (3)$$

The subscripts i and k label the radical and the nuclear spins, respectively. g_i is the g -factor of the i th radical; $a_{i,k}$ represents the hyperfine coupling constant of the k th nuclear spin in the i th radical. All other variables have their usual meanings. \hat{K} accounts for spin selective recombination processes, that is, the formation of the exciplex or the ground-state reactants with the combined rate k_S and the triplet excited state of MAnt with rate k_T

$$\hat{K}\hat{\rho}(t) = - \sum_{j=\{S,T\}} \frac{k_j}{2} [\hat{P}_j, \hat{\rho}(t)]_+ \quad (4)$$

where \hat{P}_S and \hat{P}_T are the singlet and triplet projection operator, respectively. Note that in the context of this work, k_S and k_T are effective rate constants that account for the elementary process as well as the chain dynamics controlling the approach of the reactants. Singlet–triplet dephasing (rate k_{ST}) is accounted for by⁴⁷

$$\hat{R}\hat{\rho}(t) = -k_{ST}(\hat{P}_S \hat{\rho}(t) \hat{P}_T + \hat{P}_T \hat{\rho}(t) \hat{P}_S) \quad (5)$$

We do not explicitly treat spin relaxation as these incoherent processes are not expected to be relevant on the timescale of tens of nanoseconds but we include an abstract decay time (of the order of a typical relaxation time, i.e., several hundreds of nanoseconds), τ_{sc} , to effectively eliminate the contribution of radicals that are too long-lived to remain spin correlated.

Because of the geometric growth of the dimension of eq 1 with the number of nuclear spins in the two radicals (see eq 3), a numerical solution is challenging for all but the simplest radical pairs. For this reason, we here invoke the semiclassical approximation to solve eq 1 for the accumulated density operator $\hat{\rho} = \int_0^\infty dt \rho(t)$.^{18,56,57} Details of this approach are summarized in the Supporting Information. The singlet yield is then given by

$$Y_S(B_0) = k_S \text{Tr}(\hat{P}_S \hat{\rho}(B_0)) \quad (6)$$

Assuming that the exciplex emission results from a field-independent contribution φ_0 and a field dependent contribution related to eq 6 by $\varphi_1 Y_S(B_0)$, the MFE is eventually calculated from

$$\chi(B_0) = \frac{Y_S(B_0) - Y_S(B_0 = 0)}{Y_S(B_0 = 0) + c} \quad (7)$$

where $c = \varphi_0/\varphi_1$ is a constant larger than zero.

Using DFT-derived hyperfine coupling constants (summarized Tables S1 and S2 in the Supporting Information) and a few assumptions on the typical size of pertinent parameters,

the outlined model can account for the field-dependence of the exciplex emission of the MAnt-(CH₂)_n-O-CH₂-CH₂-DMA compounds with $n \geq 8$. Figure 6 shows the fits to the

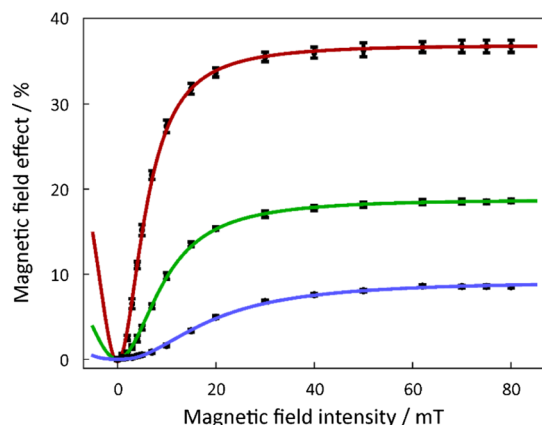


Figure 6. Simulations of the MARY curves of MAnt-*n*-O-2-DMA with $n = 8$ (blue), 10 (green), 16 (red) based on the semiclassical model outlined in the main text and the parameter values as reported in Table 1.

experimental MFEs obtained by systematically varying the singlet recombination rate constant k_S , the singlet–triplet dephasing rate k_{ST} and c . Here, $J_{av} \approx 0$ mT was assumed as the MARY curves do not show discernible minima that could be accounted for by S–T_±-mixing. In addition, we have assumed that k_T significantly exceeds k_S (in practice, we used $k_T = 10k_S$). This choice can be rationalized by observing that the triplet recombination occurs in the Marcus-normal region, while the singlet recombination is expected to be relatively slow.⁸ This is attributed to the back ET being located deep in the inverted region, and the fact that the exciplex formation is tied to more stringent requirements with respect to the stacking of the reactants than simple outer-sphere ET processes. Although the data do not allow the determination of k_T , it is noteworthy that the choice $k_S = k_T$ did not provide a convincing agreement with the experimental data. Further, $\tau_{sc} = 250$ ns was used, which corresponds to the spin relaxation times expected for organic radicals in solutions.⁵⁸ The difference in g -factors was neglected as it is too small to elicit discernible effects at the low magnetic field intensities employed here. With these choices, the MFEs can be well-modeled as is obvious from Figure 6. The fitting parameters are summarized in Table 1 and reveal a singlet recombination rate of $k_S \approx 0.1$ – 0.2 ns⁻¹. While $k_S^{-1} \approx 10$ ns for $n = 16$ and $n = 8$, we find $k_S^{-1} \approx 5$ ns for $n = 10$. In addition, $c = \varphi_0/\varphi_1$ is smallest for $n = 10$. The found recombination rates also justify our initial choice of refraining from an explicit modeling of spin relaxation. This is

Table 1. Parameters Used to Model the Magnetic Field Dependence of the Exciplex Emission Intensity of MAnt-(CH₂)_n-O-CH₂-CH₂-DMA Compounds in BN^a

parameter	k_S/s^{-1}	k_{ST}/s^{-1}	c	χ for $c = 0$ (at 75 mT)
$n = 16$	1.0×10^8	8×10^6	0.29	0.63
$n = 10$	2.0×10^8	2.1×10^8	0.21	0.25
$n = 8$	1.0×10^8	2.1×10^9	1.1	0.23

^aUncertainties: $\pm 0.4 \times 10^8$ s⁻¹ for k_S , $\pm 10\%$ for the other parameters except for k_{ST} at $n = 16$, for which the indicated value is an estimate of the order of magnitude.

due to the modulation of (predominantly) the HFIs by rotational diffusion, which do not impact the MFEs on the short timescales relevant here. On the other hand, singlet–triplet dephasing as resulting from the modulation of the exchange coupling is found to be essential to model the width of the MARY lines. k_{ST} increases strongly with decreasing n . For $n = 8$, the singlet–triplet coherence dephases on the time-scale of nanoseconds. At the same time, c increases, suggesting that tightly bound (e.g., stacked) configurations are sampled at a much higher rate for this compound than its homologs of larger n . In Table 1 we also summarize the MFE for $c = 0$, that is, for the hypothetical scenario that the exciplex is exclusively formed via magnetosensitive RIPs. With regard to these data, it is interesting to note that the small MFEs for $n = 8$ are not the result of exceedingly fast singlet–triplet dephasing but a larger propensity to form the exciplex via field-independent channels.

Although this approach is obviously valid for the compounds with $n \geq 8$, the results are less convincing for $n = 6$, as is shown in the Supporting Information (Figure S3). While the model qualitatively accounts for the dip in the MFEs once the average exchange interaction is increased to $|J_{av}| \approx 5$ mT, the predicted curve levels off too fast to fully account for the experimental saturation behavior. The best agreement is found for $k_{ST} \approx 1$ ns⁻¹, $k_S \approx 0.1$ ns⁻¹, and $c \approx 12$. Interestingly, increasing k_{ST} decreases the agreement with the experimental data by predominantly flattening out the negative dip, rather than substantially increasing the (too small) linewidth. On the basis of this observation, we suggest that the broader magnetic field response observed for the $n = 6$ compound is likely due to strain in J_{av} rather than due to increased singlet–triplet dephasing. In particular, contributions from configurations with larger exchange coupling, that is, $|J_{av}| \approx 10$ mT, appear to be significant. Several interconverting populations of radical pairs with variable $J(r)$ will have to be invoked to model the experimental data well; however, this is beyond the scope of this paper. Eventually, note that, based on an analysis summarized in ref 8, the exchange interaction is expected to be negative for the studied compounds.

MFEs on the Locally Excited Fluorophore. In several systems, the MFE on the fluorophore is accompanied by a comparable MFE on the locally excited fluorophore. This originates from the fully reversible inter-conversion between RIP, exciplex, and locally excited fluorophore.^{7,8} Energetic factors, in particular, the free energy gap between the exciplex and the fluorophore (Figure 1), determine the exciplex–fluorophore reversibility. MFEs on the locally excited fluorophores have been shown to be significant for the systems characterized by an electron-transfer free-energy difference up to $\Delta G_{ET} = -0.35$ eV, approximately.^{7,8} Assuming that the free energy of charge separation of the intramolecular systems is comparable to that for the freely diffusing DMAnt/DMA ($\Delta G_{ET} = -0.28$ eV), MFEs on the locally excited fluorophore are expected. Figure 7 shows the results of wavelength-resolved MFE measurements of the MAnt-*n*-O-2-DMA ($n = 8, 10, 16$) in BN. These action-spectra have been obtained from the emission spectra in the absence and presence of a saturating magnetic field ($B_0 = 75$ mT), $I(B_0 = 75$ mT) and $I(B_0 = 0$ mT), by calculating $\chi = I(B_0 = 75$ mT)/ $I(B_0 = 0$ mT) – 1; five scans in the presence and absence of the external magnetic field have been recorded alternately and averaged. All spectral data have been background corrected.

As argued before, these MFEs on the locally excited fluorophore can neither be attributed to triplet–triplet

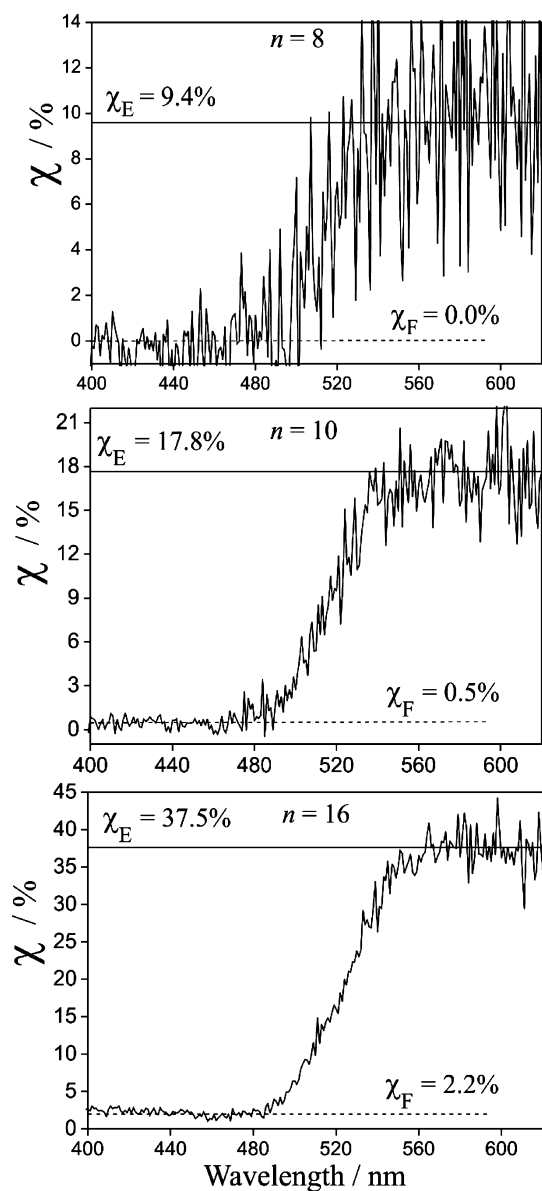


Figure 7. Wavelength-resolved MFEs of the MAn-*n*-O-2-DMA ($n = 8, 10, 16$) systems in BN. χ_F and χ_E denote the MFEs on the locally excited fluorophore and the exciplex, respectively.

annihilation (P-type delayed fluorescence) nor thermal repopulation from the triplet state (E-type).⁵⁹ The former is insignificant under the low-light, low-concentration conditions employed in the experimental condition. The latter can be excluded because the energy gap between the singlet and triplet states is large ($\Delta G_{ST} = 1.3$ eV).^{7,8} For MAn-16-O-2-DMA, the MFE on the exciplex is large ($\chi_E = 37.5\%$), and the reversible interconversion of the exciplex and locally excited fluorophore is easily recognizable ($\chi_F = 2.2\%$). The MFE on the locally excited fluorophore of the MAn-10-O-2-DMA system is 0.5%, whereas that of the MAn-8-O-2-DMA system is absent (smaller than 0.1%). If we assume a fast equilibrium of the exciplex and the locally excited fluorophore–quencher pair, a naive argument suggests that the equilibrium constant of exciplex formation is proportional to $(\chi_E/\chi_F)(I_E(B_0 = 0)/I_F(B_0 = 0))$. If we further assume that the radiative rate constants of the exciplex and the locally excited fluorophore are comparable in all compounds, we can use this quantity as measure of the

reversibility constant. For the studied compounds, both the ratio of χ_F/χ_E and I_F/I_E decrease with decreasing chain length, suggesting that the free energy gap between the exciplex and the locally excited fluorophore–quencher pair increased in the same direction. In particular, assuming that the free energy of the locally excited fluorophore state is unaltered by the length of the linker (as suggested by the invariant emission spectra of the locally excited fluorophores), this observation leads us to suggest that the exciplex is more stabilized for the shorter chain. Likely this is a consequence of an intrinsic alteration of the exciplexes, that is, a different way of stacking of the aromatic rings, or an entropic effect. The entropy of exciplex formation from the locally excited fluorophore–quencher pair is expected to be more negative for the longer chained compound, as the phase space volume corresponding to open configurations increases. This has, in fact, been found (together with an accompanying change in energy) for a similar intermolecular exciplex system with 9 and 11 bridge atoms.²³ On the other hand, ring strain is unlikely to be the cause of the observed free-energy changes, as the strain does not change much with the ring size for the large cycles at question.⁸⁰ The change in free energy is also reflected in the emission spectra of the exciplexes, which are hypsochromically shifted as n increases (see Figures S1 and S2 in the Supporting Information). Furthermore, the solvent dependence of the exciplex emission maximum shows that the degree of charge transfer is larger in the short-chain exciplexes, that is, they resemble the ion pair more.

CONCLUSIONS

MFEs on the intramolecular exciplex fluorescence have been studied for the new class of compounds MAn-*n*-O-2-DMA ($n = 6, 8, 10, 16$). The effects are interpreted in terms of the hyperfine and S/T₊-level crossing mechanisms, in which the magnetic field affects the S–T conversion within the RIP by altering the energy gap of singlet and triplet states. The MFE of the exciplex exhibits a strong dependence on the static dielectric constants, ϵ_s , of the solvent. It initially increases with increasing polarity of the solvent, attains a maximum at $\epsilon_s \approx 25$, and eventually decreases for larger solvent polarity. The solvent dependence of the MFE on the exciplex was discussed based on the effect of the solvent polarity on the separation and reencounter dynamics of the RIP and the partitioning of the quenching pathways giving way to the exciplex and the RIP, respectively. The size of the MFEs correlate strongly with the edge-to-edge distance (r) of the two radicals. The largest effect was observed for the long-chain derivative MAn-16-O-2-DMA ($\chi_E = 37.5\%$ at 75 mT). For $n = 8, 10$, and 16, the average exchange coupling is negligible and the singlet and triplet states of the RIP are nearly degenerate for most of their coherent lifetime. Simulations of the MARY lineshape in BN using the semiclassical theory reveal singlet recombination rates of the order of 0.1 ns⁻¹ and various degrees of singlet–triplet dephasing depending on the chain length. For $n = 6$, the singlet–triplet conversion is impeded at $B_0 = 0$ by a nonzero average exchange coupling of $|J_{av}| \approx 5$ mT. In this case, a dip in the fluorescence intensity results from S–T₊-mixing at intermediate magnetic field intensities. MFEs on the locally excited fluorophores have been shown to be significant for the long-chain systems ($n = 10, 16$). This observation can be attributed to the fully reversible interconversion between RIP, exciplex, and locally excited fluorophore due to a small free energy gap between the exciplex and the excited fluorophore

quencher pair. Our result suggests that the driving force of exciplex formation from the locally excited fluorophore quencher pair increases with decreasing chain length.

EXPERIMENTAL SECTION

Synthesis of Chain-Linked Fluorophore–Quencher Systems. Exemplary procedure for 2-[4-(*N,N*-dimethylamino)phenyl]ethyl 10-[9-(10-methyl)anthryl]decyl ether (MAnt-10-*O*-2-DMA): 1-bromo-10-[9-(10-methyl)anthryl]decane (MAnt-10-Br, 0.65 g, 1.58 mmole) and 2-[4-(dimethylamino)phenyl]ethanol (0.56 g, 3.39 mmole) were added to the solution of 0.57 g NaH (60% oil suspension) in *N,N*-dimethylacetamide (15 mL). The mixture was stirred for 4 h in an ice bath at 273 K. The resulting mixture was extracted with benzene (3 × 15 mL). The combined benzene phases were washed by cold water (3 × 20 mL) and dried over MgSO₄. The solvent was removed in vacuo. The product was isolated by column chromatography on silica gel with *n*-hexane and an *n*-hexane/ethyl acetate mixture (95:5) as the eluting solvent to obtain MAnt-10-*O*-2-DMA (0.25 g, 38% yield). Formula: C₃₅H₄₅ON, melting point: 328–329 K. ¹H NMR (CDCl₃, 500 MHz): δ 8.6–7.4 ppm (8H, protons of the anthracene moiety), 7.2–6.7 (4H, protons of benzene ring), 3.7–3.5 (4H, –CH₂–O–CH₂–), 3.45 (2H, –CH₂–DMA), 3.1 (3H, CH₃–anthracene), 2.95 (6H, (CH₃)₂N–), 2.8 (2H, –CH₂–anthracene), 2.0–1.2 (16H, protons of the chain). ¹³C NMR (CDCl₃, 125 MHz): δ 134–122 ppm (20C, aromatic carbons), 70–74 (4C, –CH₂–O–CH₂– and –N(CH₃)₂), 35–36 (3C, CH₃–anthracene, –CH₂–anthracene and –CH₂–benzene), 14–32 (8C, methylene carbons). MS (EI) *m/z*: 495.35 (M⁺, 100). The linked fluorophore–quencher pairs of different chain lengths (MAnt-*n*-*O*-2-DMA, *n* = 6, 8, 16) were prepared by an analogous procedure. See the Supporting Information for synthetic details including the preparation of precursors.

Solvents and Sample Preparation. Solvent mixtures of PA (Aldrich 99.5%, distilled under reduced pressure, ε_s = 6) and BN (BN, Fluka 99%, distilled under reduced pressure, ε_s = 24.7) allow for a systematic variation of the dielectric constant ε_s in the range from 6 to 24.7 (295 K). Mixtures of different ε_s values were prepared observing that ε_s = w_{PA}ε_{PA} + (1 – w_{PA})ε_{BN}, where w_{PA} is the weight fraction of PA.^{9–11} For these mixtures, the viscosity (η) and the refractive index (*n*) are almost independent of solvent composition. Furthermore, the Pekar factor (1/*n*² – 1/ε_s = 0.456 for ε_s = 15), which governs the outer-sphere ET reorganization energy and thus the rate of ET processes, varies by only ±5% in the studied ε_s range.^{9,45,61,62} In addition, neat propionitrile (EtCN, Aldrich 99.5%, distilled under reduced pressure, ε_s = 28.3) and AN (Aldrich 99.8%, distilled under reduced pressure, ε_s = 36.0) are used to extend the range of solvent polarities. The concentration of ether-linked fluorophore–quencher pairs was 2 × 10^{–5} M. Samples were prepared in septa-sealed quartz cuvettes. To remove dissolved oxygen, all solutions were bubbled with nitrogen for 15 min prior to measurements.

Steady-State MFE Measurements. The MFEs on the intramolecular exciplex emission were obtained by using the experimental setup described in refs.^{9,11} The exciplex luminescence intensity was recorded at 550 nm, whereas the fluorophore moiety was excited continuously at 374 nm. The fluorescence intensity was sampled three times in the absence and presence of an additional external magnetic field; the two conditions were alternated and each was acquired for 60 s. All

measurements were conducted at 295 K. Fluorescence signals have been background-corrected. The three repetitions were analyzed independently and the experimental errors were estimated according to the method described in refs.^{9,11} The MFE is defined as the relative change of the fluorescence intensity of the exciplex, I_E(λ_{em}, B₀), in the presence of an external magnetic field relative to the zero-field scenario. It was evaluated from

$$\chi_E = \frac{I_E(\lambda_{em}, B_0) - I_E(\lambda_{em}, B_0 = 0)}{I_E(\lambda_{em}, B_0 = 0)} = \frac{\bar{I}(\lambda_{em}, B_0) - \bar{I}(\lambda_{em}, B_0 = 0)}{\bar{I}(\lambda_{em}, B_0 = 0) - (\bar{I}_F(\lambda_{em}, B_0 = 0) - \overline{BG}(\lambda_{em}))I_c/I_0 - \overline{BG}(\lambda_{em})} \quad (8)$$

Here, $\bar{I}(\lambda_{em}, B_0)$ and $\bar{I}(\lambda_{em}, B_0 = 0)$ are the mean intensities sampled over the 60 s intervals at λ_{em} in a saturating magnetic field (B₀) and in the absence (B₀ = 0) of an additional external magnetic field, respectively. $\bar{I}_F(\lambda_{em}, B_0 = 0)$ is the residual emission of the locally excited fluorophore at the emission wavelength λ_{em} in the absence of quencher. I_c and I₀ are the emission intensities of the locally excited fluorophore in the presence and absence of the quencher, respectively, which have been obtained from the decomposition of the spectrally resolved fluorescence spectra in contributions from the fluorophore and the exciplex. $\overline{BG}(\lambda_{em})$ is the mean background intensity recorded for a sample of only the solvent. The subtractive term in the denominator accounts for the residual fluorescence of the locally excited fluorophore at the wavelength used to monitor the exciplex emission. I₀ has been determined from spectra of the dimethyl anthracene recorded under the same experimental conditions and for the same concentration as used in the actual experiments. This correction is crucial for intermolecular exciplexes in polar solutions, for which the exciplex emission is small.

ASSOCIATED CONTENT

Supporting Information

The Supporting Information is available free of charge on the ACS Publications website at DOI: 10.1021/acsomega.8b01232.

Extracted exciplex spectra, solvent dependence of the maxima of exciplex emission, solution of eq 1 in the semiclassical limit, DFT-derived hyperfine coupling constants, tentative simulations of the MARY curve of MAnt-6-*O*-2-DMA, and detailed description of the synthesis of the polymethylene ether-linked donor–acceptor compounds (PDF)

AUTHOR INFORMATION

Corresponding Author

*E-mail: d.r.kattnig@exeter.ac.uk. Phone: +44 (0) 1392 72 7479.

ORCID

Daniel R. Kattnig: 0000-0003-4236-2627

Notes

The authors declare no competing financial interest.

ACKNOWLEDGMENTS

The financial support from The Royal Society (RG170378), Ho Chi Minh City University of Technology and Education (T2018-36TĐ) and Austrian Science Fund (FWF-Project P

21518-N19) is gratefully acknowledged. D.R.K. is thankful NVIDIA for supporting this research through their GPU Grant Program.

REFERENCES

- (1) Henbest, K. B.; Kukura, P.; Rodgers, C. T.; Hore, P. J.; Timmel, C. R. Radio frequency magnetic field effects on a radical recombination reaction: a diagnostic test for the radical pair mechanism. *J. Am. Chem. Soc.* **2004**, *126*, 8102–8103.
- (2) Rodgers, C. T.; Norman, S. A.; Henbest, K. B.; Timmel, C. R.; Hore, P. J. Determination of radical re-encounter probability distributions from magnetic field effects on reaction yields. *J. Am. Chem. Soc.* **2007**, *129*, 6746–6755.
- (3) Justinek, M.; Grampp, G.; Landgraf, S.; Hore, P. J.; Lukzen, N. N. Electron self-exchange kinetics determined by MARY spectroscopy: theory and experiment. *J. Am. Chem. Soc.* **2004**, *126*, 5635–5646.
- (4) Lukzen, N. N.; Kattinig, D. R.; Grampp, G. The effect of signs of hyperfine coupling constant on MARY spectra affected by degenerate electron exchange. *Chem. Phys. Lett.* **2005**, *413*, 118–122.
- (5) Pal, K.; Kattinig, D. R.; Grampp, G.; Landgraf, S. Experimental observation of preferential solvation on a radical ion pair using MARY spectroscopy. *Phys. Chem. Chem. Phys.* **2012**, *14*, 3155–3161.
- (6) Pal, K.; Grampp, G.; Kattinig, D. R. Solvation dynamics of a radical ion pair in micro-heterogeneous binary solvents: a semi-quantitative study utilizing MARY line-broadening experiments. *ChemPhysChem* **2013**, *14*, 3389–3399.
- (7) Kattinig, D. R.; Rosspeintner, A.; Grampp, G. Fully reversible interconversion between locally excited fluorophore, exciplex, and radical ion pair demonstrated by a new magnetic field effect. *Angew. Chem., Int. Ed.* **2008**, *47*, 960–962.
- (8) Kattinig, D. R.; Rosspeintner, A.; Grampp, G. Magnetic field effects on exciplex-forming systems: the effect on the locally excited fluorophore and its dependence on free energy. *Phys. Chem. Chem. Phys.* **2011**, *13*, 3446–3460.
- (9) Richert, S.; Rosspeintner, A.; Landgraf, S.; Grampp, G.; Vauthey, E.; Kattinig, D. R. Time-resolved magnetic field effects distinguish loose ion pairs from exciplexes. *J. Am. Chem. Soc.* **2013**, *135*, 15144–15152.
- (10) Hoang, H. M.; Pham, T. B. V.; Grampp, G.; Kattinig, D. R. Exciplexes versus loose ion pairs: how does the driving force impact the initial product ratio of photoinduced charge separation reactions? *J. Phys. Chem. Lett.* **2014**, *5*, 3188–3194.
- (11) Pham, V. T. B.; Hoang, H. M.; Grampp, G.; Kattinig, D. R. Effects of preferential solvation revealed by time-resolved magnetic field effects. *J. Phys. Chem. B* **2017**, *121*, 2677–2683.
- (12) Aich, S.; Basu, S. Magnetic Field Effect: A tool for identification of spin state in a photoinduced electron-transfer reaction. *J. Phys. Chem. A* **1998**, *102*, 722–729.
- (13) Werner, U.; Staerk, H. Magnetic field effect in the recombination reaction of radical ion pairs: dependence on solvent dielectric constant. *J. Phys. Chem.* **1995**, *99*, 248–254.
- (14) Chowdhury, M.; Dutta, R.; Basu, S.; Nath, D. Magnetic field effect on exciplex luminescence in liquids. *J. Mol. Liq.* **1993**, *57*, 195–228.
- (15) Melnikov, A. R.; Davydova, M. P.; Sherin, P. S.; Korolev, V. V.; Stepanov, A. A.; Kalneus, E. V.; Benassi, E.; Vasilevsky, S. F.; Stass, D. V. X-ray generated recombination exciplexes of substituted diphenylacetylenes with tertiary amines: a versatile experimental vehicle for targeted creation of deep-blue electroluminescent systems. *J. Phys. Chem. A* **2018**, *122*, 1235–1252.
- (16) Melnikov, A. R.; Verkhovlyuk, V. N.; Kalneus, E. V.; Korolev, V. V.; Borovkov, V. I.; Sherin, P. S.; Davydova, M. P.; Vasilevsky, S. F.; Stass, D. V. Estimation of the fraction of spin-correlated radical ion pairs in irradiated alkanes using magnetosensitive recombination luminescence from exciplexes generated upon recombination of a probe pair. *Z. Phys. Chem.* **2017**, *231*, 239.
- (17) Steiner, U. E.; Ulrich, T. Magnetic field effects in chemical kinetics and related phenomena. *Chem. Rev.* **1989**, *89*, 51–147.
- (18) Salikhov, K. M.; Molin, I. N.; Buchachenko, A. L. *Spin Polarization and Magnetic Effects in Radical Reactions*; Elsevier: Budapest, 1984; pp 117–140.
- (19) Closs, G. L. Mechanism explaining nuclear spin polarizations in radical combination reactions. *J. Am. Chem. Soc.* **1969**, *91*, 4552–4554.
- (20) Sengupta, T.; Choudhury, S. D.; Basu, S. Medium-Dependent Electron and H Atom Transfer between 2'-Deoxyadenosine and Menadione: A Magnetic Field Effect Study. *J. Am. Chem. Soc.* **2004**, *126*, 10589–10593.
- (21) Koch, M.; Letrun, R.; Vauthey, E. Exciplex formation in bimolecular photoinduced electron-transfer investigated by ultrafast time-resolved infrared spectroscopy. *J. Am. Chem. Soc.* **2014**, *136*, 4066–4074.
- (22) Dereka, B.; Koch, M.; Vauthey, E. Looking at photoinduced charge transfer processes in the IR: answers to several long-standing questions. *Acc. Chem. Res.* **2017**, *50*, 426–434.
- (23) Vanderauwera, P.; DeSchryver, F. C.; Weller, A.; Winnik, M. A.; Zachariasse, K. A. Intramolecular exciplex formation and fluorescence quenching as a function of chain length in omega-dimethylaminoalkyl esters of 2-anthracenecarboxylic acid. *J. Phys. Chem.* **1984**, *88*, 2964–2970.
- (24) O'Dea, A. R.; Curtis, A. F.; Green, N. J. B.; Timmel, C. R.; Hore, P. J. Influence of dipolar interactions on radical pair recombination reactions subject to weak magnetic fields. *J. Phys. Chem. A* **2005**, *109*, 869–873.
- (25) Tero-Kubota, S. Singlet and triplet energy splitting in the radical ion pairs generated by photoinduced electron-transfer reactions. *Pure Appl. Chem.* **2001**, *73*, 519–523.
- (26) Staerk, H.; Busmann, H.-G.; Kühnle, W.; Weller, A. Solvent effects on the magnetic-field-dependent reaction yields of photo-generated radical ion pairs. *Chem. Phys. Lett.* **1989**, *155*, 603–608.
- (27) Nath, D. N.; Chowdhury, M. Effect of variation of dielectric constant on the magnetic field modulation of exciplex luminescence. *Pramana* **1990**, *34*, 51–66.
- (28) Petrov, N. K.; Shushin, A. I.; Frankevich, E. L. Solvent effect on magnetic field modulation of exciplex fluorescence in polar solutions. *Chem. Phys. Lett.* **1981**, *82*, 339–343.
- (29) Suppan, P. Local polarity of solvent mixtures in the field of electronically excited molecules and exciplexes. *J. Chem. Soc., Faraday Trans. 1* **1987**, *83*, 495–509.
- (30) Busmann, H.-G.; Staerk, H.; Weller, A. Solvent influence on the magnetic field effect of polymethylene-linked photogenerated radical ion pairs. *J. Chem. Phys.* **1989**, *91*, 4098–4105.
- (31) Staerk, H.; Kühnle, W.; Treichel, R.; Weller, A. Magnetic field dependence of intramolecular exciplex formation in polymethylene-linked A-D systems. *Chem. Phys. Lett.* **1985**, *118*, 19–24.
- (32) Basu, S.; Nath, D.; Chowdhury, M.; Winnik, M. A. Magnetic field effects in a polymer-chain-linked donor-acceptor system. *Chem. Phys.* **1992**, *162*, 145–153.
- (33) Tanimoto, Y.; Hasegawa, K.; Okada, N.; Itoh, M.; Iwai, K.; Sugioka, K.; Takemura, F.; Nakagaki, R.; Nagakura, S. Magnetic field effects on the intra- and intermolecular exciplex fluorescence of phenanthrene and dimethylaniline. *J. Phys. Chem.* **1989**, *93*, 3586–3594.
- (34) Tanimoto, Y.; Okada, N.; Itoh, M.; Iwai, K.; Sugioka, K.; Takemura, F.; Nakagaki, R.; Nagakura, S. Magnetic field effects on the fluorescence of intramolecular electron-donor-acceptor systems. *Chem. Phys. Lett.* **1987**, *136*, 42–46.
- (35) Cao, H.; Fujiwara, Y.; Haino, T.; Fukazawa, Y.; Tung, C.-H.; Tanimoto, Y. Magnetic Field Effects on Intramolecular Exciplex Fluorescence of Chain-Linked Phenanthrene and N,N-Dimethylaniline: Influence of Chain Length, Solvent, and Temperature. *Bull. Chem. Soc. Jpn.* **1996**, *69*, 2801–2813.
- (36) Cao, H.; Miyata, K.; Tamura, T.; Fujiwara, Y.; Tanimoto, Y.; Okazaki, M.; Iwai, K.; Yamamoto, M. Effect of a high magnetic field on the decay rate of chain-linked intramolecular exciplex fluorescence. *Chem. Phys. Lett.* **1995**, *246*, 171–175.

- (37) Cao, H.; Miyata, K.; Tamura, T.; Fujiwara, Y.; Katsuki, A.; Tung, C.-H.; Tanimoto, Y. Effects of high magnetic field on the intramolecular exciplex fluorescence of chain-linked phenanthrene and dimethylaniline. *J. Phys. Chem. A* **1997**, *101*, 407–411.
- (38) De, R.; Fujiwara, Y.; Haino, T.; Tanimoto, Y. Effect of high magnetic fields on intramolecular exciplex fluorescence of pyrene and dimethylaniline systems. *Chem. Phys. Lett.* **1999**, *315*, 383–389.
- (39) Petrov, N. K.; Alfimov, M. V.; Budyka, M. F.; Gavrishova, T. N.; Staerk, H. Intramolecular electron hopping in double carbazole molecules studied by the fluorescence-detected magnetic field effect. *J. Phys. Chem. A* **1999**, *103*, 9601–9604.
- (40) Werner, U.; Kuehnle, W.; Staerk, H. Magnetic field dependent reaction yields from radical ion pairs linked by a partially rigid aliphatic chain. *J. Phys. Chem.* **1993**, *97*, 9280–9287.
- (41) Murakami, M.; Maeda, K.; Arai, T. Dynamics of intramolecular electron transfer reaction of FAD studied by magnetic field effects on transient absorption spectra. *J. Phys. Chem. A* **2005**, *109*, 5793–5800.
- (42) Klein, J. H.; Schmidt, D.; Steiner, U. E.; Lambert, C. Complete monitoring of coherent and incoherent spin flip domains in the recombination of charge-separated states of donor-iridium complex-acceptor triads. *J. Am. Chem. Soc.* **2015**, *137*, 11011–11021.
- (43) Zollitsch, T. M.; Jarocho, L. E.; Bialas, C.; Henbest, K. B.; Kodali, G.; Dutton, P. L.; Moser, C. C.; Timmel, C. R.; Hore, P. J.; Mackenzie, S. R. Magnetically sensitive radical photochemistry of non-natural flavoproteins. *J. Am. Chem. Soc.* **2018**, *140*, 8705–8713.
- (44) Paul, S.; Kiryutin, A. S.; Guo, J.; Ivanov, K. L.; Matysik, J.; Yurkovskaya, A. V.; Wang, X. Magnetic field effect in natural cryptochrome explored with model compound. *Sci. Rep.* **2017**, *7*, 1.
- (45) Kuzmin, M. G.; Soboleva, I. V.; Dolotova, E. V. The behavior of exciplex decay processes and interplay of radiationless transition and preliminary reorganization mechanisms of electron transfer in loose and tight pairs of reactants. *J. Phys. Chem. A* **2007**, *111*, 206–215.
- (46) Basu, S.; Nath, D. N.; Chowdhury, M. Time-resolved studies of the effect of a magnetic field on exciplex luminescence. *Chem. Phys. Lett.* **1989**, *161*, 449–454.
- (47) Shushin, A. I. The effect of the spin exchange interaction on SNP and RYDMR spectra of geminate radical pairs. *Chem. Phys. Lett.* **1991**, *181*, 274–278.
- (48) Murai, H.; Kuwata, K. CIDEP of transient radical-ion pair: Photolysis of N,N,N',N'-tetramethyl-p-phenylenediamine in 2-propanol. *Chem. Phys. Lett.* **1989**, *164*, 567–570.
- (49) de Kanter, F. J. J.; den Hollander, J. A.; Huizer, A. H.; Kaptein, R. Biradical CIDNP and the dynamics of polymethylene chains. *Mol. Phys.* **1977**, *34*, 857–874.
- (50) Kubo, R. Stochastic Liouville equations. *J. Math. Phys.* **1963**, *4*, 174–183.
- (51) Bittl, R.; Schulten, K. Biradical spin dynamics with distance-dependent exchange interaction and electron transfer efficiency. *Chem. Phys. Lett.* **1990**, *173*, 387–392.
- (52) Parmon, V. N.; Kokorin, A. I.; Zhidomirov, G. M. Conformational structure of nitroxide biradicals use of biradicals as spin probes. *J. Struct. Chem.* **1977**, *18*, 104–147.
- (53) Grampp, G.; Rasmussen, K.; Kokorin, A. I. Intramolecular spin exchange in flexible short-chain biradicals in solutions with various viscosity. *Appl. Magn. Reson.* **2004**, *26*, 245–252.
- (54) Mladenova-Kattinig, B.; Grampp, G.; Kokorin, A. I. Influence of pressure on intramolecular dynamics in a long-chain flexible nitroxide biradical. *Appl. Magn. Reson.* **2015**, *46*, 1359–1366.
- (55) Kattinig, D. R.; Sowa, J. K.; Solov'yov, I. A.; Hore, P. J. Electron spin relaxation can enhance the performance of a cryptochrome-based magnetic compass sensor. *New J. Phys.* **2016**, *18*, 063007.
- (56) Schulten, K.; Wolynes, P. G. Semiclassical description of electron spin motion in radicals including the effect of electron hopping. *J. Chem. Phys.* **1978**, *68*, 3292–3297.
- (57) Miura, T.; Maeda, K.; Arai, T. The spin mixing process of a radical pair in low magnetic field observed by transient absorption detected nanosecond pulsed magnetic field effect. *J. Phys. Chem. A* **2006**, *110*, 4151–4156.
- (58) Evans, E. W.; Kattinig, D. R.; Henbest, K. B.; Hore, P. J.; Mackenzie, S. R.; Timmel, C. R. Sub-millitesla magnetic field effects on the recombination reaction of flavin and ascorbic acid radicals. *J. Chem. Phys.* **2016**, *145*, 085101.
- (59) Birks, J. B. *Photophysics of Aromatic Molecules*, 2nd ed.; Wiley-Interscience: New York, 1970; pp 355–371.
- (60) Dragojlovic, V. Conformational analysis of cycloalkanes. *ChemTexts* **2015**, *1*, 14.
- (61) Marcus, R. A. On the Theory of Oxidation-Reduction Reactions Involving Electron Transfer. I. *J. Chem. Phys.* **1956**, *24*, 966–978.
- (62) Marcus, R. A.; Sutin, N. Electron transfers in chemistry and biology. *Biochim. Biophys. Acta, Rev. Bioenerg.* **1985**, *811*, 265–322.